RESEARCH DEPARTMENT REPORT SERIES no. 57/2007 ISSN 1749-8775

PLEISTOCENE SEDIMENTS FROM THE TRENT VALLEY OPTICALLY STIMULATED LUMINESCENCE (OSL) DATING

SCIENTIFIC DATING REPORT

Jean-Luc Schwenninger, David R Bridgland, Andy J Howard and Tom White

ARCHAEOLOGICAL SCIENCE

ENGLISH HERITAGE

Research Department Report Series 57/2007

Pleistocene Sediments from the Trent Valley Optically Stimulated Luminescence (OSL) Dating

Jean-Luc Schwenninger, David R Bridgland, Andy J Howard and Tom White

ISSN 1749-8775

Research Department Report Series 57/2007

Pleistocene Sediments from the Trent Valley Optically Stimulated Luminescence (OSL) Dating

Jean-Luc Schwenninger[1], David R Bridgland[2], Andy J Howard[3] and Tom White[2]

Summary

A total of 33 samples were collected from 16 different sites within the Trent Valley for dating by optically stimulated luminescence (OSL). Luminescence age estimates were obtained from sand-sized quartz grains and palaeodose determinations were made using a single aliquot regenerative-dose (SAR) measurement protocol. The environmental dose rate for each sample was calculated using the results of elemental analysis by ICP-MS and in situ gamma-ray spectroscopy measurements. The concentrations of radioactive elements within the sediments were well above detection limits but the quartz used for dating was often characterized by low sensitivity to laboratory induced irradiation. This problem combined with the common occurrence of contaminant feldspar minerals provided challenging conditions for luminescence dating. Despite these limitations, meaningful age estimates could be obtained for the majority of samples and the results provide a much improved and robust chronological framework for terrace development and landscape evolution of the Middle and Lower Trent Valley.

Keywords

Optically Stimulated Luminescence
Pleistocene
Geochronology

Author's Address

[1]Research Laboratory for Archaeology and the History of Art, University of Oxford, 6 Keble Road, Oxford OX1 3QJ

[2]Department of Geography, University of Durham, Science Laboratories, South Road, Durham DH1 3LE

[3]The Institute of Archaeology & Antiquity, The University of Birmingham, Edgbaston, Birmingham, B15 2TT

Pleistocene sediments from the Trent Valley
Optically stimulated luminescence (OSL) dating

Jean-Luc Schwenninger[1], David R. Bridgland[2], Andy J. Howard[3] and Tom White[2]

[1]Research Laboratory for Archaeology and the History of Art, University of Oxford, Dyson Perrins Building, South Parks Road, Oxford OX1 3QY

[2]Department of Geography, University of Durham, Science Laboratories, South Road, Durham ,DH1 3LE

[3]The Institute of Archaeology & Antiquity, The University of Birmingham, Edgbaston, Birmingham, B15 2TT

Summary: A total of 33 samples were collected from 16 different sites within the Trent Valley for dating by optically stimulated luminescence (OSL). Luminescence age estimates were obtained from sand-sized quartz grains and palaeodose determinations were made using a single aliquot regenerative-dose (SAR) measurement protocol. The environmental dose rate for each sample was calculated using the results of elemental analysis by ICP-MS and *in situ* gamma-ray spectroscopy measurements. The concentrations of radioactive elements within the sediments were well above detection limits but the quartz used for dating was often characterized by low sensitivity to laboratory induced irradiation. This problem combined with the common occurrence of contaminant feldspar minerals provided challenging conditions for luminescence dating. Despite these limitations, meaningful age estimates could be obtained for the majority of samples and the results provide a much improved and robust chronological framework for terrace development and landscape evolution of the Middle and Lower Trent Valley.

Keywords:
Pleistocene
Geochronology
Optically Stimulated Luminescence dating

1 Introduction

1.1 General

An extensive record of Pleistocene sediments is preserved within the catchment area over the river Trent (Fig 1.1) which is one of the most northerly rivers in Europe to have yielded significant assemblages of Palaeolithic artefacts (Wymer 1999; Howard and Knight 2004). The Trent Valley is also one of the most important aggregate areas in the UK and intensive mineral extraction is resulting in the continuing loss of important archaeological resources and sites of scientific interest.

These aggregate deposits are known to contain Lower and Middle Palaeolithic artefacts and biological remains but the differentiation and until recently, dating of such deposits remained uncertain and poorly understood. A key objective of the ALSF funded Trent Valley Palaeolithic Project (TVPP) was to test the validity of the existing model of terrace development (see Fig 1.2) and to refine the chrono-stratigraphic sequence of such deposits within the study area by securing samples for dating by optically stimulated luminescence (OSL). The existing classification of terrace units is based on a revised mapping of the region by the British Geological Survey (Brandon and Sumbler 1988; 1991) but relies heavily on observed stratigraphic relationships in the field or biostratigraphy as opposed to absolute dating. Optical dating allows us to determine when certain mineral grains were last exposed to daylight. In recent years, this method has been successfully applied to Pleistocene fluvial deposits in southern England (Briant *et al* 2006; Schwenninger *et al* 2006; Toms *et al* 2005). Thus an important objective was to assess if such novel techniques would work on glaciofluvial sediments elsewhere and could help improve our understanding and knowledge of the Palaeolithic towards the more northern fringes of known early human occupation in the British Isles.

For this purpose, a series of 33 samples (Table 1.1) were collected from key sedimentary units at 16 different sites (Figs 1.3–1.8) located within the Middle and Lower drainage system of the present and former Trent. Most samples were obtained from exposed sections inside active quarries, disused sand pits or from artificial cuttings associated with irrigation ponds. On a few occasions, samples were also secured from hand or machine excavated trenches.

In situ gamma dose rate measurements using an EG&G Ortec MicroNomad NaI gamma-ray spectrometer were made for every sample except for X2626. The environmental dose rate required for the calculation of the OSL age estimates was obtained from these direct radiation measurements (gamma dose rate) as well as further complementary laboratory based geochemical analysis of sub-samples. The concentrations of radioactive elements were determined by ICP-MS using a fusion preparation method. These results were only used to determine the contribution of the beta dose rate to the total environmental dose received by the sample. Sample processing and OSL measurements were made at the Oxford Luminescence Dating Laboratory, Research Laboratory for Archaeology & the History of Art, University of Oxford. Further details regarding individual samples are presented in Table 1.1 and Appendix 1.

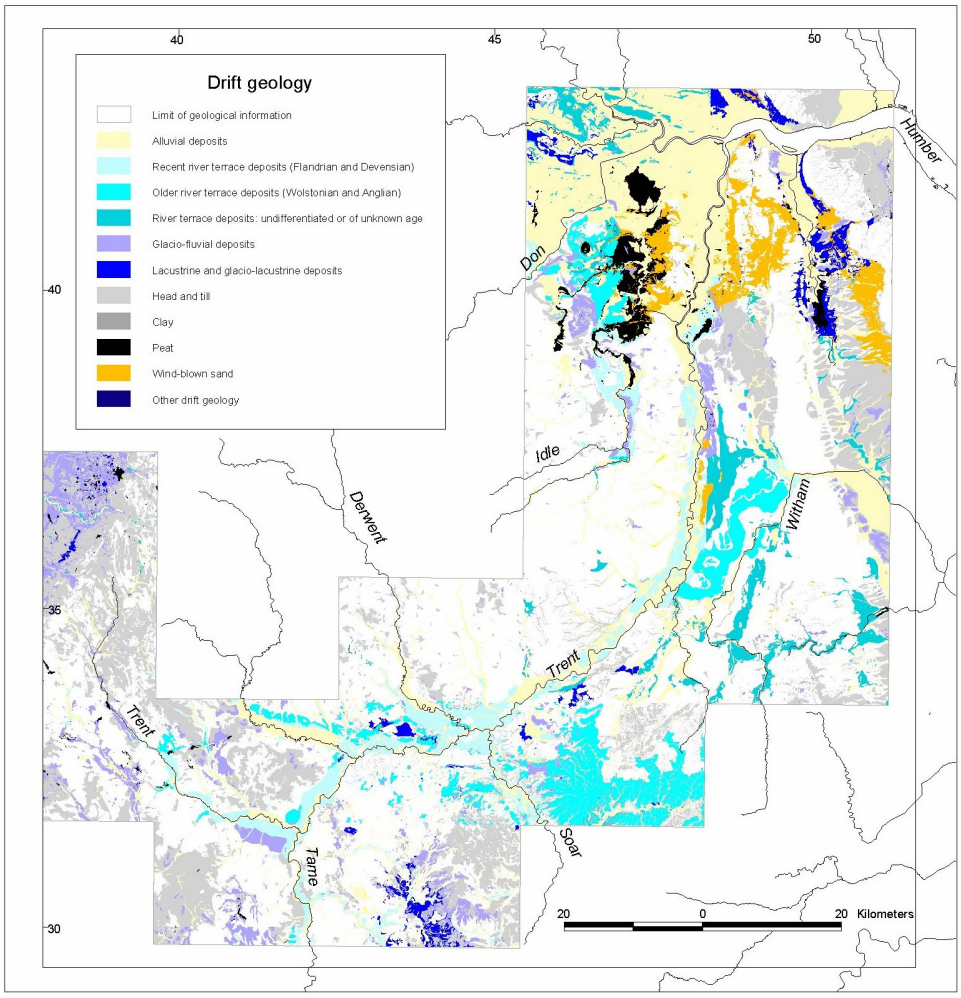

Figure 1.1 Map of the Trent Valley study area featuring major types of surface deposits (from Knight and Howard 2004)

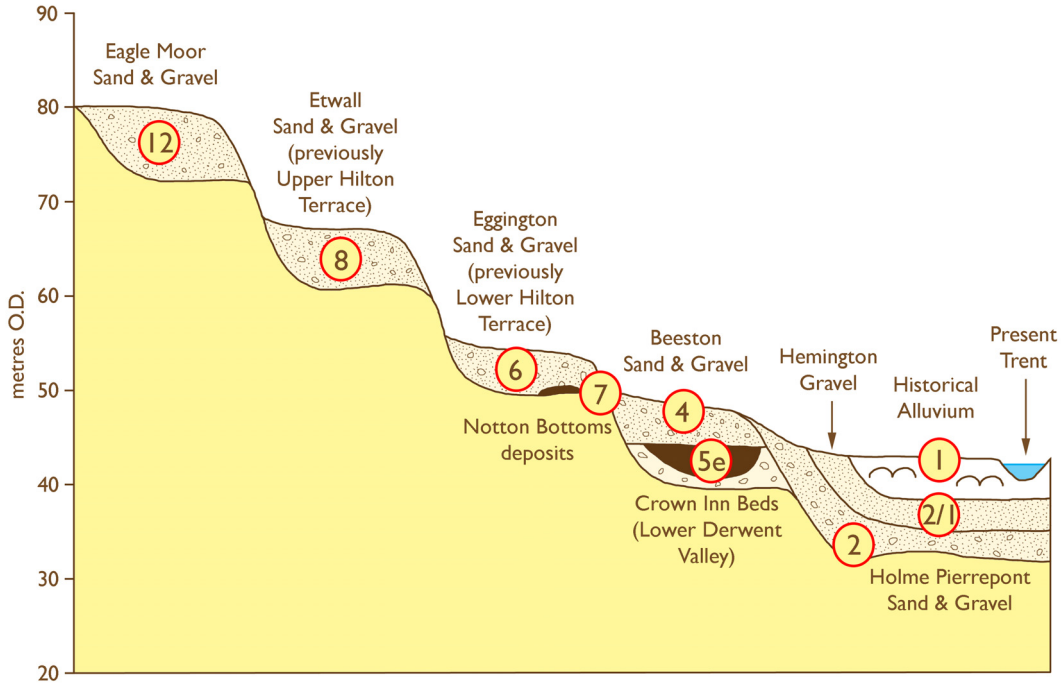

Figure 1.2 Schematic representation of the Middle Trent terrace sequence (after Bridgland *et al* 2006)

OSL sampling at Birch Holt Farm Irrigation Pond [BHF05-01]

Birch Holt Farm [BHF05-01]

OSL sampling at Norton Disney Quarry [NOD05-02]

Norton Disney Quarry [NOD05-03]

Norton Disney Quarry [NOD05-02]

Figure 1.3 OSL sampling locations

Norton Disney Quarry [NOD05-03]

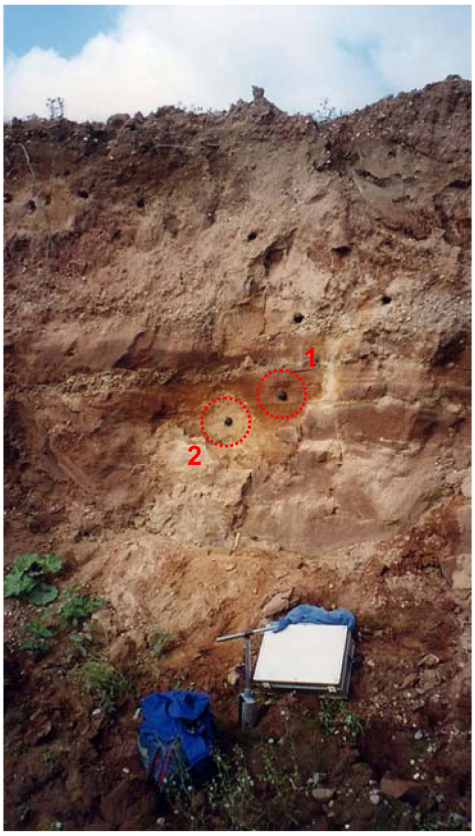

East Leake Quarry [ELQ05-01& 02]

East Leake Quarry [ELQ05-03A&B replicates]

Hanson Quarry [HUN05-01]

Figure 1.4 OSL sampling locations

Wellsyke Farm [WEL05-01]

Whisby Quarry [WHI05-02]

Whisby Quarry [WHI05-01]

Kirkby-on-Bain Quarry [KOB05-01& 02]

Figure 1.5 OSL sampling locations

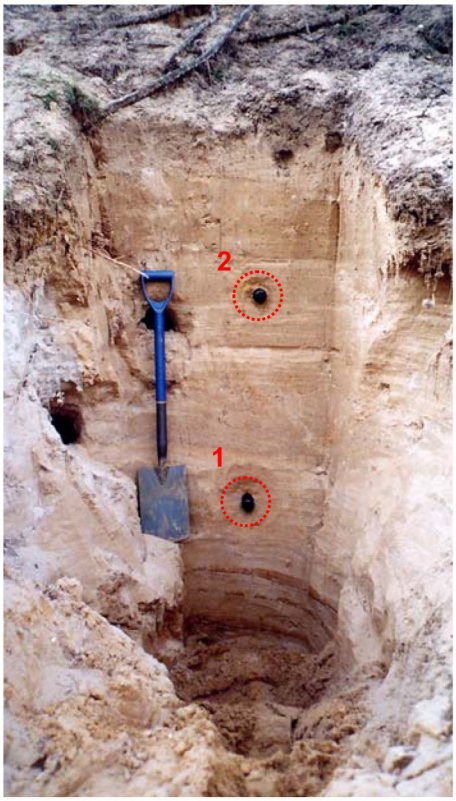

Foxhill Pit [FOX05-01 & 02]

South Scarle Irrigation Pond [SCI05-01& 02]

Langford Quarry [LAN05-01 & 02]

Tattershall-Thorpe Quarry [TAT05-01]

Figure 1.6 OSL sampling locations

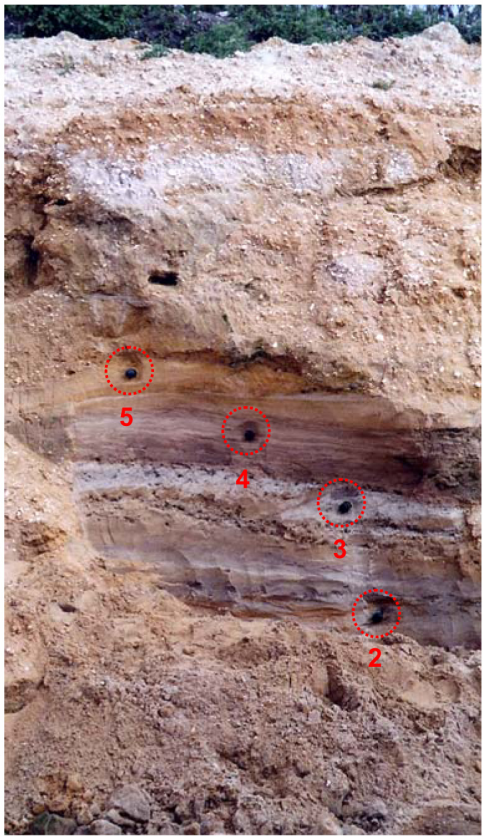

Tattershall-Thorpe Quarry [TAT05-02, 03, 04, & 05]

Willington Quarry [WIL05-01 & 02]

Atkins Farm [ATK05-01 & 02]

Girton Quarry [GIR05-01]

Figure 1.7 OSL sampling locations

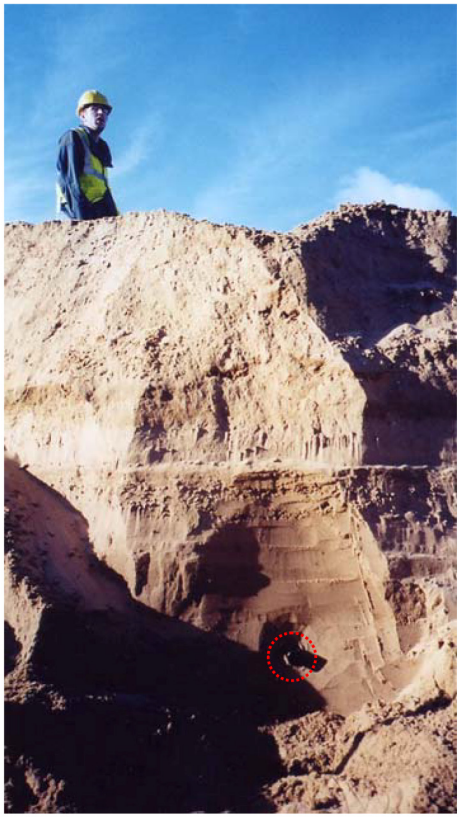

Girton Quarry [GIR05-02]

Besthorpe Quarry [BES05-01]

Figure 1.8 OSL sampling locations

Field code	Lab code	Site name	Altitude	*In situ* NaI γ-spectrometry
ELQ05-01	X2570	East Leake Quarry (RMC) [SK556250]	70	Yes
ELQ05-02	X2571	East Leake Quarry (RMC)	70	Yes
ELQ05-03A	X2572	East Leake Quarry (RMC)	70	Yes
ELQ05-03B	X2573	East Leake Quarry (RMC)	70	Yes
BHF05-01	X2574	Birch Holt Farm Irrigation Pond [SK866607]	10	Yes
NOD05-01	X2575	Norton Disney [SK887598]	10	Yes
NOD05-02	X2576	Norton Disney	10	Yes
NOD05-03	X2577	Norton Disney	10	Yes
HUN05-01	X2593	Hanson Quarry [SK199156]	50	Yes
WHI05-01	X2594	Whisby Quarry [SK896670]	10	Yes
WHI05-02	X2595	Whisby Quarry	10	Yes
KOB05-01	X2596	Kirkby-on-Bain [TF236604]	10	Yes
KOB05-02	X2597	Kirkby-on-Bain	10	Yes
WEL05-01	X2598	Welsyke Farm [TF232637]	30	Yes
FOX05-01	X2616	Foxhill Pit [TF228624]	20	Yes
FOX05-02	X2617	Foxhill Pit	20	Yes
LAN05-01	X2618	Langford Quarry [SK810603]	10	Yes
LAN05-02	X2619	Langford Quarry	10	Yes
SCI05-01	X2620	South Scarle Irrigation Pond [SK856639]	10	Yes
SCI05-02	X2621	South Scarle Irrigation Pond	10	Yes
TAT05-01	X2622	Tattershall-Thorpe (RMC) [TF207608]	5	Yes
TAT05-02	X2623	Tattershall-Thorpe (RMC)	5	Yes
TAT05-03	X2624	Tattershall-Thorpe (RMC)	5	Yes
TAT05-04	X2625	Tattershall-Thorpe (RMC)	5	Yes
TAT05-05	X2626	Tattershall-Thorpe (RMC)	5	No
ATK05-01	X2660	Atkins Farm [SK330298]	55	Yes
ATK05-02	X2661	Atkins Farm	55	Yes
BAR05-01	X2662	Barrow on Trent Quarry [SK344275]	30	Yes
BES05-01	X2663	Besthorpe Quarry [SK817626]	10	Yes
GIR05-01	X2664	Girton Quarry [SK827683]	5	Yes
GIR05-02	X2665	Girton Quarry	5	Yes
WIL05-01	X2666	Willington Quarry [SK279278]	40	Yes
WIL05-02	X2667	Willington Quarry	40	Yes

Table 1.1 OSL sample details. A total of 33 samples were collected from relevant stratigraphic units at 16 sites located within the present and former Trent drainage area. Further details regarding individual samples may be found in Appendix 1

2 Methods

2.1 The physical basis of luminescence dating

When ionising radiation (predominantly alpha, beta, or gamma radiation) interacts with an insulating crystal lattice (such as quartz or feldspar), a net redistribution of electronic charge takes place. Electrons are stripped from the outer shells of atoms and though most return immediately, a proportion escape and become trapped at meta-stable sites within the lattice. This charge redistribution continues for the duration of the radiation exposure and the amount of trapped charge is therefore related to both the

duration and the intensity of radiation exposure. Even though trapped at meta-stable sites, electrons become 'free' if the crystal is subjected to heat or exposed to light. Once liberated, a free electron may become trapped once again or may return to a vacant position caused by the absence of a previously displaced electron (a 'hole'). This latter occurrence is termed 'recombination' and the location of the hole is described as the 'recombination centre'. As recombination occurs, a proportion of the energy of the electron is dissipated. Depending upon the nature of the centre where recombination occurs, this energy is expelled as heat and/or light. Therefore, when the crystal grain is either heated or illuminated following natural or artificial laboratory irradiation (the 'dose') the total amount of light emitted (luminescence) is directly related to the number of liberated electrons and available recombination sites. This is the fundamental principle upon which luminescence dating is based. A more detailed account of the method may be found in Aitken (1998).

In cases where the duration of dosing is not known (as is the case for dating), estimates can be made from laboratory measurements. The response (the sensitivity) of the sample to radiation dose (ie the amount of light observed for a given amount of laboratory radiation, usually β-radiation) must be established. From this relationship the equivalent radiation exposure required to produce the same amount of light as that observed following the natural environmental dose can be determined, and is termed the palaeodose or 'equivalent dose' (D_e). The palaeodose (measured in Gy) is therefore an estimate of the total dose absorbed during the irradiation period. When the dose rate (the amount of radiation per unit time, measured in μGy/a) is measured (or calculated from measured concentrations of radionuclides), the duration of the dosing period can be calculated using the equation:

$$\text{Duration of dosing period (Age)} = \text{Palaeodose} \div \text{dose rate}$$

The technique of optical dating was first applied to quartz by Huntley *et al* (1985), and methodological details were further developed by Smith *et al* (1986) and Rhodes (1988). The technique was demonstrated to work well for aeolian samples by Smith *et al* (1990), and has further proved to provide useful age estimates for a range of sedimentary contexts ranging from aeolian (eg Stokes *et al* 1997) to glacial contexts (Owen *et al* 1997). Further developmental research has introduced palaeodose measurement protocols that use a 'single aliquot regenerative-dose' (SAR) protocol (Murray and Wintle 2000). These protocols generally have the potential to provide improved accuracy (eg through correction of sensitivity change, interpolation rather than extrapolation of D_e values) as well as increased precision. In some cases they may also provide an indication of incomplete zeroing of the luminescence signal at the time of deposition. Recent research within the laboratory (Rhodes *et al* 2003) has demonstrated the high precision and accuracy that may be achieved with this technique.

2.2 Sample preparation

The laboratory procedures were designed to yield pure quartz, of a particular grain size range, from the natural sediment samples. In order to obtain this material, samples were taken through a standard preparation procedure, as outlined below. All laboratory treatments were performed under low intensity laboratory safe-lighting, from purpose-built filtered sodium lamps (emitting at 588nm).

After removal of the exposed ends of the sampling containers, the unexposed central portion of the sample was wet-sieved and the 180–255µm grain size was used for dating (see Appendix 1 for details of specific samples). The chosen fraction was treated with hydrochloric acid (HCl) to remove carbonate and then treated in concentrated HF (48%) for 100 minutes. This treatment serves two purposes: (i) to dissolve feldspar grains, and (ii) to remove (etch) the outer surface of quartz grains (the only part of each quartz grain exposed during burial to natural alpha radiation). Any heavy minerals present were subsequently removed by gravity separation using a sodium polytungstate solution at 2.68 $g.cm^{-3}$. Finally, each sample was re-sieved to remove heavily etched grains. The order of the heavy liquid separation and second sieving are on occasion reversed for practical reasons, and for samples with extremely low yields, either or both of these treatments may be omitted after careful consideration. The prepared quartz samples were mounted on 1cm diameter aluminium discs for luminescence measurement using viscous silicone oil.

Various tests for sample purity are made. Sub-samples of the prepared material are examined using optical microscopy and the sample is exposed (within the Risø measurement system) to infrared (IR) light. Quartz generally does not produce measurable IR luminescence at room temperature whereas feldspar, which can suffer from anomalous fading of the infrared stimulated luminescence (IRSL) and OSL signals, or may be less rapidly bleached in some environments, produces an intense luminescence when stimulated with IR. A strong IRSL signal was detected for most samples from the Trent Valley and therefore the prepared quartz grains were treated for ~ 2–3 weeks in concentrated H_2SiF_6 (silica-saturated HF) in order to effectively dissolve non-quartz material. Following this treatment, a small IRSL (see Table 3.2) persisted but this was negligible relative to the OSL signal and any interference with the luminescence signal of quartz was further reduced by adopting a post-IR blue OSL measurement procedure (Banerjee *et al*/2001.). This is designed to deplete any feldspar contribution to the OSL signal, by preceding each OSL measurement with an IRSL measurement. The IR exposure reduces the size of feldspar contributions.

In order to determine the attenuating effect of pore water on the environmental dose rate of the sediments, additional samples were collected in the field and hermetically sealed. The moisture content of the sample was determined in the laboratory by weighing the sample before and after oven drying at 50°C.

2.3 The single aliquot regenerative-dose (SAR) protocol

The SAR method is a regeneration procedure where the light level of the natural signal is converted into Gy via an interpolation between regenerated (ie known dose) points. The natural and regenerated signals are measured using the same aliquot. Sensitivity change commonly observed in quartz TL/OSL has previously precluded meaningful results being obtained this way. A key development reported by Murray and Wintle (2000) is that sample (aliquot) sensitivity is monitored following each OSL measurement (L_i) using the OSL response to a common test dose (S_i). Plots of L_i / S_i provide the necessary (sensitivity change corrected) data for interpolation. The procedure is further outlined in Figure 2.1.

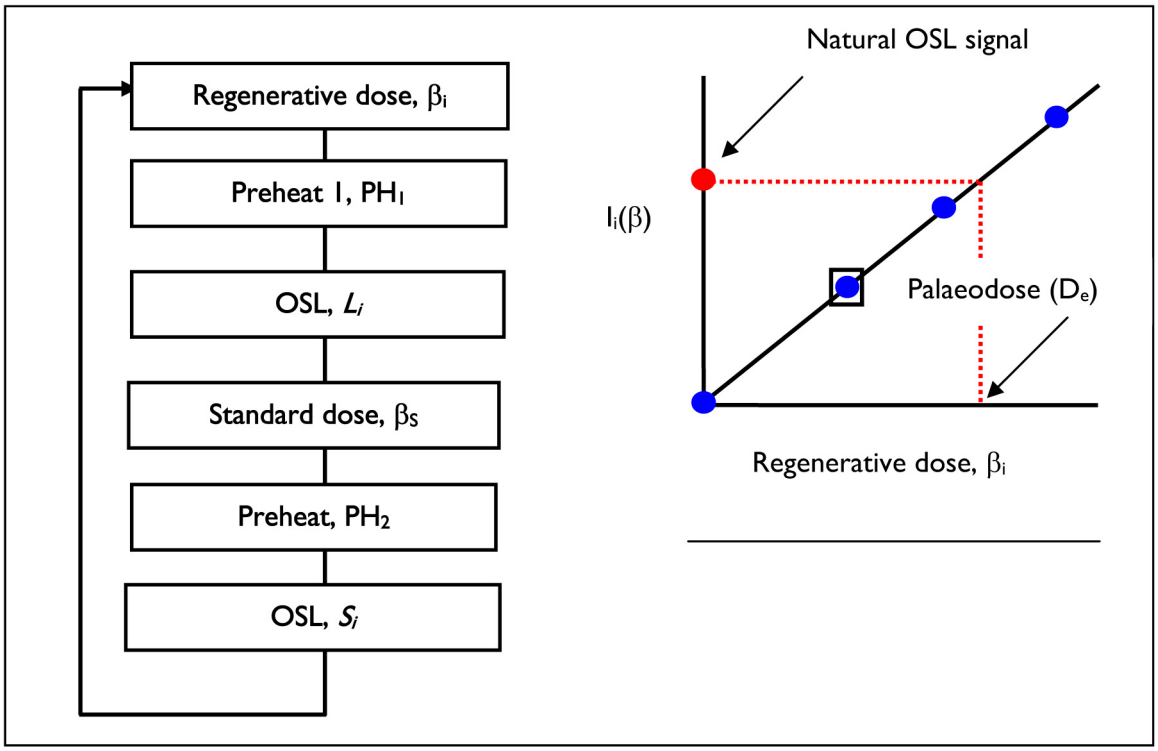

Figure 2.1 The SAR method. The procedure illustrated here is described in further detail in the text

Steps 1–6 are repeated *n* times in order to produce the data points required for interpolation (the first dose β_1 being zero, to give a measure of the natural signal). Typically n=7 (ie the natural plus 6 regeneration points, including one zero dose point and one repeat point). PH_1 and PH_2 are usually different although Murray and Wintle (2000) report no dependence of the palaeodose on either (over the range of 200–280°C). The OSL signal is integrated over the initial part of the decay (to ~10% of initial intensity) and the background is taken as the light level measured at the end of each OSL measurement.

Murray and Wintle (2000) have introduced two further steps in to the measurement procedure. The first is the re-measurement of the first regenerated data point (indicated by the box in the explanatory Fig 2.1 above). The ratio of the two points (the "recycling ratio") provides an assessment of the efficacy of the sensitivity correction and the accuracy of the technique (large differences being suggestive of an ineffective technique). The recycling ratio (ideally unity) is typically in the range 0.95–1.05. The second additional step is a measurement of the regenerated OSL due to zero dose. This value gives a measure of the degree of thermal transfer to the trap(s) responsible for OSL during pre-heating. The ratio of this value to the natural OSL value (both corrected for sensitivity change) gives the "thermal transfer ratio" and ideally this should be in the range of 0.005–0.020.

2.4 Measurement procedures and conditions

Luminescence measurements were made using automated Risø luminescence measurement equipment. There are currently three different systems within the Luminescence Dating Laboratory that can be used for routine dating, the major difference between them being the optical stimulation sources. In two systems, optical excitation is provided by filtered blue diodes (emitting ~410–510nm), and in the third a filtered Halogen lamp (emitting ~420–560nm) is used. In all three systems, infrared stimulation is also provided using either an array of IR diodes or a single IR laser diode (depending on the measurement system). Luminescence is detected in the UV region on all systems, using EMI 9635Q bialkali photomultiplier tubes, filtered with Hoya U340 glass filters. Sample irradiation is provided in all cases by sealed ^{90}Sr sources at a rate of 1.5–3 Gy/minute depending on the system used.

The mean palaeodose for each sample was obtained from series of six to 12 individual aliquots (see Appendix 3 for further details regarding the statistics used in palaeodose and error calculations). All OSL measurements were made at 125°C (to ensure no re-trapping of charge to the 110°C TL trap during measurement) for between 50 and 100s, depending on the measurement system used. The signal detected in the initial 1 to 5 seconds (with the stable background count rate from the last 10 to 25 seconds subtracted) was corrected for sensitivity using the OSL signal regenerated by a subsequent beta dose (β_s). To ensure removal of unstable OSL components, removal of dose quenching effects, and to stimulate re-trapping and ensure meaningful comparison between naturally and laboratory irradiated signals, pre-heating was performed prior to each OSL measurement. Following each regenerative dose (β_i) and the natural dose, a pre-heat (PH_1) at 260°C for 10s was used. Following each test dose (β_s), a pre-heat (PH_2) of 220°C for 10s was applied (see Section 2.3 for further details of the SAR method). All the OSL measurements incorporated a post-IR blue OSL stage in which each OSL measurement is preceded by an IRSL measurement at 50°C, to reduce the effects of any residual feldspar grains (Banerjee *et al*/2001) but the SAR procedure is otherwise unchanged.

For every sample, a routine internal laboratory procedure referred to as DELIA (D_e Luminescence Initial Assessment) was applied prior to the main SAR measurement in order to determine their approximate palaeodose value. This consisted in the use of a simplified version of the SAR measurement protocol applied to a limited number of three test discs in order to determine the internal variability, the OSL and TL signal form and sensitivity, as well as the magnitude of any IRSL signals. This considerably assists in the optimal selection of regenerative and test dose values, number of aliquots to measure, and the preheat combination selected. Most quartz samples showed high levels of IRSL at this stage and were given an extended (2–3 weeks) treatment in fluorosilicic acid (H_2SiF_6).

3 Results and discussion

The OSL dating results including age estimates, palaeodose, and environmental dose rate measurements are summarized in Table 3.2. More specific criteria describing the characteristics of the luminescence data are presented in Table 3.3 and further details regarding individual samples may be found in Appendix 1. Factors affecting the dose rate determinations and the statistics used in error calculations are described in more detail in Appendices 2 and 3.

As mentioned above, most samples were characterized by a high infrared signal response which is generally considered to be indicative of contamination by feldspathic mineral grains. Extended treatment with fluorosilicic acid for periods up to three weeks enabled to reduce the IRSL signal to acceptable levels (Table 3.3). As a further precaution, all the luminescence measurements were done using a post-IR blue measurement protocol (Banerjee *et al* 2001). In addition to tests (Table 3.3) for the recycling ratio (repeat measurement of a sensitivity corrected SAR dose point) and thermal transfer (measurement of the zero dose point) which are routinely carried out as part of the SAR procedure, eight samples were also selected for dose recovery tests (Wintle and Murray 2006). Three unheated aliquots were prepared for each sample following the removal of the natural trapped charge electron population (bleached with blue LED's for 100sec at room temperature) and then given a laboratory dose of 1000sec. Since a known dose is given to the sample, the ability of the SAR measurement protocol can be tested directly. A summary of these results is presented below in Table 3.1.

Sample	Mean recovered dose	Dose recovery ratio
X2570	1063.3 ±64.18	0.94
X2574	978.1 ±16.90	1.02
X2597	952.9 ±107.48	1.05
X2619	978.1 ±31.84	1.02
X2621	957.4 ±34.87	1.04
X2622	1069.1 ±88.35	0.93
X2662	993.3 ±142.73	1.01
X2664	987.2 ±67.03	1.01
		Mean: 1.00

Table 3.1 Summary of dose recovery tests performed for a selected number of prepared quartz samples from sites in the Trent Valley. These had their natural signal removed through bleaching with blue LED light at room temperature and were then given a 1000sec laboratory dose prior to luminescence measurements using a modified SAR protocol

Field code	Laboratory code	Palaeodose (Gy)	Dose rate (Gy/ka)	OSL age estimate (ka)
ELQ05-01	X2570	263.56 ±18.90	1.25 ±0.09	212 ±22
ELQ05-02	X2571	[193.70 ±33.40]	1.47 ±0.12	[132 ±25] very unreliable
ELQ05-03A	X2572	252.14 ±15.66	1.45 ±0.11	174 ±17
ELQ05-03B	X2573	218.08 ±17.55	1.49 ±0.12	147 ±17
BHF05-01	X2574	26.07 ±2.22	1.62 ±0.12	16.1 ±1.9
NOD05-01	X2575	133.02 ±17.86	1.26 ±0.10	106 ±17
NOD05-02	X2576	190.89 ±12.03	1.77 ±0.15	108 ±12
NOD05-03	X2577	132.85 ±7.43	1.09 ±0.08	122 ±12
HUN05-01	X2593	55.82 ±5.94	2.31 ±0.22	24.2 ±3.5
WHI05-01	X2594	58.35 ±6.54	1.05 ±0.08	55.4 ±7.6
WHI05-02	X2595	51.88 ±2.91	1.66 ±0.13	31.3 ±3.0
KOB05-01	X2596	26.96 ±3.94	1.02 ±0.08	26.5 ±4.4
KOB05-02	X2597	36.83 ±4.77	1.09 ±0.08	33.7 ±5.0
WEL05-01	X2598	260.23 ±13.76	1.46 ±0.12	178 ±18
FOX05-01	X2616	247.30 ±6.82	1.34 ±0.07	185 ±12
FOX05-02	X2617	259.08 ±8.77	1.47 ±0.08	177 ±12
LAN05-01	X2618	38.54 ±2.83	1.25 ±0.09	30.8 ±3.3
LAN05-02	X2619	38.70 ±1.79	1.38 ±0.12	27.9 ±2.8
SCI05-01	X2620	93.37 ±8.28	1.48 ±0.12	62.9 ±7.5
SCI05-02	X2621	57.97 ±10.96	1.28 ±0.10	45.2 ±9.3
TAT05-01	X2622	122.65 ±5.41	1.06 ±0.08	116 ±10.4
TAT05-02	X2623	159.19 ±6.91	1.02 ±0.07	156 ±13.0
TAT05-03	X2624	142.11 ±19.91	1.06 ±0.07	133 ±21.0
TAT05-04	X2625	197.25 ±15.68	2.02 ±0.17	98.9 ±11.6
TAT05-05	X2626	146.22 ±12.28	1.30 ±0.14	112 ±16
ATK05-01	X2660	[250]	1.68 ±0.12	[149] very unreliable
ATK05-02	X2661	[120]	1.52 ±0.10	[102] very unreliable
BAR05-01	X2662	16.92 ±4.26	1.55 ±0.13	10.9 ±2.9
BES05-01	X2663	28.77 ±2.81	1.14 ±0.10	25.3 ±3.3
GIR05-01	X2664	20.64 ±1.34	1.09 ±0.08	18.9 ±1.9
GIR05-02	X2665	23.58 ±1.15	1.12 ±0.08	21.0 ±1.9
WIL05-01	X2666	53.10 ±5.93	1.20 ±0.09	44.3 ±5.9
WIL05-02	X2667	48.45 ±5.32	1.26 ±0.10	38.5 ±5.2

Table 3.2 Summary of OSL dating results. The results are based on luminescence measurements of sand-sized quartz (90–125 or 180–255μm). All samples were measured using a SAR post-IR blue OSL protocol (Murray and Wintle 2000; Banerjee *et al* 2001). Dose rate calculations are based on *in situ* radioactivity measurements (gamma dose rate) combined with laboratory based ICP-MS analysis of the concentration of radioactive elements (potassium, thorium and uranium) to calculate the beta dose rate. For sample X2626 *in situ* γ-ray spectrometer measurement was made and the mean gamma dose of the four associated samples was used for dose rate evaluation. The final OSL age estimates include an additional 2% systematic error to account for uncertainties in source calibration. Dose rate calculations are based on Aitken (1985). These incorporated beta attenuation factors (Mejdahl 1979), dose rate conversion factors (Adamiec and Aitken 1998), and an absorption coefficient for the water content (Zimmerman 1971). The contribution of cosmic radiation to the total dose rate was calculated as a function of latitude, altitude, burial depth and average over-burden density based on data by Prescott and Hutton (1994). Further details regarding individual samples may be found in Appendix 1

Field code	Laboratory code	Mean IRSL/OSL ratio	Mean recycling ration	Mean thermal transfer (%)	Rejected aliquots (%)
ELQ05-01	X2570	0.06	1.04	6.2	*33*
ELQ05-02	X2571	0.07	0.94	6.7	*50*
ELQ05-03A	X2572	0.07	0.99	3.9	*33*
ELQ05-03B	X2573	0.16	1.03	3.6	17
BHF05-01	X2574	0.17	1.10	11.1	17
NOD05-01	X2575	0.06	1.0	2.3	17
NOD05-02	X2576	0.06	1.01	2.2	*33*
NOD05-03	X2577	0.02	1.02	3.5	*33*
HUN05-01	X2593	0.03	1.05	2.9	*50*
WHI05-01	X2594	0.11	1.10	2.8	*33*
WHI05-02	X2595	0.03	*0.87*	2.9	*50*
KOB05-01	X2596	0.08	1.22	2.1	0
KOB05-02	X2597	0.04	1.07	5.6	17
WEL05-01	X2598	0.03	1.16	0.7	*50*
FOX05-01	X2616	0.02	0.97	1.1	0
FOX05-02	X2617	0.01	1.06	1.7	0
LAN05-01	X2618	0.04	1.03	11.4	17
LAN05-02	X2619	0.01	0.98	16.0	0
SCI05-01	X2620	0.04	-	4.9	17
SCI05-02	X2621	0.04	1.01	5.9	17
TAT05-01	X2622	0.02	1.04	2.9	0
TAT05-02	X2623	0.02	1.01	2.6	17
TAT05-03	X2624	0.01	0.99	1.8	0
TAT05-04	X2625	0.01	1.04	3.3	33
TAT05-05	X2626	0.02	1.02	3.3	17
ATK05-01	X2660	0.0001	0.97	4.1	*50*
ATK05-02	X2661	0.0002	1.01	7.9	*50*
BAR05-01	X2662	0.02	0.99	6.8	33
BES05-01	X2663	0.07	0.99	14.1	17
GIR05-01	X2664	0.08	1.03	15.5	0
GIR05-02	X2665	0.04	1.05	16.7	0
WIL05-01	X2666	0.07	0.99	5.9	17
WIL05-02	X2667	0.05	0.90	3.5	33

Table 3.3 Summary of luminescence characteristics including tests for feldspar contamination (following extended 2-3 week treatment with H_2SIF_6 acid), recycling, recuperation and as well as the percentage of aliquots that were rejected from the analysis

The results of the recovery tests show that the ratio of the known dose to the measured dose is very close to unity and therefore the adopted SAR measurement protocol can be considered to be working correctly. This is reassuring given the rather low sensitivity of the quartz in the majority of samples analysed here and a persisting but acceptable IR signal following sample preparation. Samples particularly affected by low sensitivity were those collected from Whisby, Kirkby-on-Bain, and Willington. Although a larger than normal test dose of 5–10Gy was used there is no indication that this had any detrimental effects on determining the palaeodose. A high degree of inter-aliquot scatter was observed among individual palaeodose estimates of certain samples. Where this is the situation it often seems to affect all the samples from the same site suggesting that the sediments may have suffered partial bleaching or mixing. This is certainly the case for both samples collected from Atkins Farm (X2660 and X2661) as well as sample X2571 from East Leake Quarry.

The observed high degree of scatter may be due to the presence of older contaminant grains with a residual geological signal or a trapped charge population maintained from a previous depositional environment. This can be minimized to some extent by preparing small aliquots (2–3mm) which effectively reduces the chances of incorporating rare contaminants among the grain population. However, in this study the low sensitivity of the quartz often imposed larger (5–8mm diameter) rather than smaller aliquot sizes. Regarding the three samples mentioned above, it is clear that no reliable age estimates may be obtained (at best, a rough minimum age may be inferred) but it is more difficult to come to a clear conclusion for those samples affected to a lesser extent by this issue.

This problem was anticipated based on previous experience gained from the dating of Pleistocene glaciofluvial sediments in the Solent (Briant *et al* 2006). In such situations, single grain measurements may enable to obtain a more detailed and better understanding of the true palaeodose distribution among the mineral grain population. Older or younger contaminants can be identified and removed from the analysis. Clearly, for those samples characterized by larger errors and having relatively high rejection rates (Table 3.2) the age estimates should be interpreted with caution and they should be considered to be preliminary (X2570-X2573, X2593, X2598, X2660, X2661). These samples would certainly benefit from further analysis before the results can be published in a scientific journal.

A further point of concern relates to the fact that the modern day moisture content of the sediments may not at all be representative of the average water content experienced by the sample through its burial period. The sandy nature of most of the sediments targeted for OSL dating implies that they drain easily and quickly and thus can experience extreme dryness during the summer season and be waterlogged in winter. Furthermore, many samples were collected from quarries where water is pumped out of the sediments to enable aggregate extraction. For this reason the modern water content cannot even be considered to represent natural conditions. In the absence of any clear indication as to what the true moisture content of the sediments may have been in the past, the calculation of the age estimates was undertaken by attaching a large inflated error margin in order to accommodate conditions from dry (5%) to near saturation levels (25%).

Despite specific problems affecting some of the samples and the difficulties caused by to the overall low sensitivity of the quartz , the ubiquitous contamination by feldspars and the uncertainty surrounding past water content, this study suggests that OSL can be successfully applied to the dating of aggregate deposits in the Trent region. The majority of OSL age estimates appear to provide meaningful results and are in broad agreement with the proposed sequence of terrace formation and landscape development.

4 References

Adamiec, G, and Aitken, M J, 1998 Dose-rate conversion factors: update, *Ancient TL*, **16**, 37–50

Aitken, M J, 1998 *Introduction to optical dating*, Oxford (Oxford University Press)

Banerjee, D, Murray, A S, Bøtter-Jensen, L, and Lang, A, 2001 Equivalent dose estimation using a single aliquot of polymineral fine grains, *Radiation Measurements*, **33**, 73–94

Brandon, A, and Sumbler, M G, 1988 An Ipswichian fluvial deposit at Fulbeck, Lincolnshire and the chronology of the Trent terraces, *J Quaternary Sci*, **3**, 127–33

Brandon, A, and Sumbler, M G, 1991 The Balderton Sand and Gravel: pre-Ipswichian cold stage fluvial deposits near Lincoln, England, *J Quaternary Sci*, **6**, 117–38

Briant, R M, Bates, M R, Schwenninger, J-L, and Wenban-Smith,F, 2006 An optically stimulated luminescence dated Middle to Late Pleistocene fluvial sequence from the western Solent Basin, southern England, *J Quaternary Sci*, **21** 507–23

Bridgland, D R, Howard, A J, White, M J, and White, T S, 2006 *The Trent Valley: archaeology and landscape of the Ice Age*, Durham (University of Durham Press)

Howard, A J, and Knight, D, 2004 The Pleistocene Background, in *Trent Valley Landscapes* (D Knight and A J Howard), Kings Lynn (Heritage Marketing and Publications Ltd)

Huntley, D J, Godfrey-Smith, D I, and Thewalt, M L W, 1985 Optical dating of sediments, *Nature*, **313**, 105–7

Knight, D, and Howard, A J, 2004 *Trent Valley Landscapes*, Kings Lynn (Heritage Marketing and Publications Ltd)

Mejdahl, V, 1979 Thermoluminescence dating: beta dose attenuation in quartz grains, *Archaeometry*, **21**, 61–73

Murray, A S, and Wintle, A G, 2000 Luminescence dating of quartz using an improved single-aliquot regenerative-dose protocol, *Radiation Measurements,* **32**, 57–73

Owen, L A, Mitchell, W A, Bailey, R M, Coxon, P, and Rhodes, E J, 1997 Style and timing of glaciation in the Lahul Himalaya, northern India: a frame work for reconstructing Late Quaternary palaeoclimatic change in the western Himalayas, *J Quaternary Sci*, **12**, 83–109

Prescott, J R, and Hutton, J T, 1994 Cosmic ray contributions to dose rates for luminescence and ESR dating: large depths and long term time variations, *Radiation Measurements,* **23**, 497–500

Rhodes, E J, 1988 Methodological considerations in the optical dating of quartz, *Quaternary Sci Rev*, **7**, 395–400

Rhodes, E J, Bronk Ramsey, C, Outram, Z, Batt, C, Willis, L, Dockrill, S, Batt, C, and Bond, J, 2003 Bayesian methods applied to the interpretation of multiple OSL dates: high precision sediment age estimates from Old Scatness Broch excavations, Shetland Isles, *Quaternary Sci Rev*, **22**, 1231–44

Schwenninger, J-L, Rhodes, E J, Bates, M R, Briant, R M, and Wenban-Smith, F, 2006 Optically stimulated luminescence (OSL) dating of Quaternary deposits from the Sussex/Hampshire coastal corridor, EH Res Dept Rep Ser, **20/2006**

Smith, B W, Aitken, M J, Rhodes, E J, Robinson, P D, and Geldard, D M, 1986 Optical dating: methodological aspects, *Radiation Protection Dosimetry,* **17**, 229–33

Smith, B W, Rhodes, E J, Stokes, S, Spooner, N A, and Aitken, M J, 1990 Optical dating of sediments: initial results from Oxford, *Archaeometry*, **32**, 19-31

Stokes, S, Thomas, D S G, and Washington R W, 1997 Multiple episodes of aridity in southern Africa since the last interglacial period, *Nature,* **388**, 154-9

Toms, P S, Hosfield, R T, Chambers, J C, Green, C P, and Marshall, P, 2005 *Optical Dating of the Broom Palaeolithic sites, Devon and Dorset*, English Heritage CfA Rep , **16/2005**

Wintle, A G, and Murray, A S, 2006 A review of quartz optically stimulated luminescence characteristics and their relevance in single-aliquot regeneration dating protocols, *Radiation Measurements*, **41**, 369–91

Wymer, J J, 1999 *The Lower Palaeolithic Occupation of Britain*, Wessex Archaeology and English Heritage

Zimmermann, D W, 1971 Thermoluminescent dating using fine grains from pottery, *Archaeometry*, **13**, 29–52

Appendix 1: Details of radioactivity data and age calculations

	East Leake	East Leake	East Leake	East Leake	Birch Holt Farm
Sample number	**ELQ05-01**	**ELQ05-02**	**ELQ05-03A**	**ELQ05-03B**	**BHF05-01**
Laboratory code	**X2570**	**X2571** Unreliable very scattered	**X2572**	**X2573**	**X2574**
Palaeodose (Gy)	263.56	*193.70*	252.14	218.08	26.07
uncertainty	19.621	33.624	16.452	18.084	2.280
measured	18.90	*33.40*	15.66	17.55	2.22
Systematic laboratory error (2 %)	5.271	3.874	5.043	4.362	0.521
Grain size					
Min. grain size (µm)	180	180	180	180	180
Max grain size (µm)	255	255	255	255	255
External gamma-dose (Gy/ka)	0.468	0.514	0.557	0.557	0.624
error	0.002	0.002	0.002	0.002	0.002
Measured concentrations					
standard fractional error	0.050	0.050	0.050	0.050	0.050
% K	0.920	1.280	1.100	1.150	1.250
error (%K)	0.046	0.064	0.055	0.058	0.063
Th (ppm)	2.600	2.100	2.700	3.000	2.100
error (ppm)	0.130	0.105	0.135	0.150	0.105
U (ppm)	0.700	0.500	0.800	0.800	0.600
error (ppm)	0.035	0.025	0.040	0.040	0.030
Cosmic dose calculations					
Depth (m)	4.800	5.200	5.000	5.000	2.400
error (m)	0.100	0.100	0.100	0.100	0.100
Average overburden density (g.cm^3)	1.900	1.900	1.900	1.900	1.900
error (g.cm^3)	0.100	0.100	0.100	0.100	0.100
Latitude (deg.), north positive	53	53	53	53	53
Longditude (deg.), east positive	1	1	1	1	1
Altitude (m above sea-level))	70	70	70	70	10
Cosmic dose rate (µGy/ka)	0.116	0.111	0.114	0.114	0.154
error	0.009	0.008	0.009	0.009	0.013
Moisture content					
Measured water content (%)	4.34	5.83	6.35	3.50	13.04
Estimated avearge water content	0.150	0.150	0.150	0.150	0.150
error	0.100	0.100	0.100	0.100	0.100
Total dose rate, Gy/ka	**1.25**	**1.47**	**1.45**	**1.49**	**1.62**
error	**0.09**	**0.12**	**0.11**	**0.12**	**0.12**
% error	**7.50**	**8.27**	**7.60**	**7.75**	**7.46**

AGE (ka)	**211.69**	**131.71**	**173.86**	**146.84**	**16.14**
error	**22.36**	**25.33**	**17.41**	**16.67**	**1.86**
% error	**10.56**	**19.23**	**10.02**	**11.35**	**11.49**

	Norton Disney	Norton Disney	Norton Disney	Hanson Quarry	Whisby Quarry
Sample number	**NOD05-01**	**NOD05-02**	**NOD05-03**	**HUN05-01**	**WHI05-01**
Laboratory code	**X2575**	**X2576**	**X2577**	**X2593**	**X2594**
Palaeodose (Gy)	133.02	190.89	132.85	55.82	58.35
uncertainty	18.057	12.621	7.891	6.044	6.643
measured	17.86	12.03	7.43	5.94	6.54
Systematic laboratory error (2 %)	2.660	3.818	2.657	1.116	1.167
Grain size					
Min. grain size (µm)	180	180	180	180	180
Max grain size (µm)	255	255	255	255	255
External gamma-dose (Gy/ka)	0.454	0.623	0.395	0.674	0.383
error	0.001	0.002	0.002	0.002	0.001
Measured concentrations					
standard fractional error	0.050	0.050	0.050	0.050	0.050
% K	1.040	1.590	0.830	2.210	0.790
error (%K)	0.052	0.080	0.042	0.111	0.040
Th (ppm)	2.100	4.400	1.900	4.700	1.700
error (ppm)	0.105	0.220	0.095	0.235	0.085
U (ppm)	0.600	1.300	0.600	1.300	0.600
error (ppm)	0.030	0.065	0.030	0.065	0.030
Cosmic dose calculations					
Depth (m)	7.000	8.500	5.000	5.250	5.000
error (m)	0.100	0.100	0.100	0.100	0.100
Average overburden density (g.cm^3)	1.900	1.900	1.900	1.900	1.900
error (g.cm^3)	0.100	0.100	0.100	0.100	0.100
Latitude (deg.), north positive	53	53	53	53	53
Longditude (deg.), east positive	1	1	1	2	1
Altitude (m above sea-level))	10	10	10	50	10
Cosmic dose rate (µGy/ka)	0.090	0.078	0.113	0.110	0.113
error	0.007	0.006	0.008	0.008	0.008
Moisture content					
Measured water content (%)	6.07	18.48	9.59	11.25	3.75
Estimated avearge water content	0.150	0.200	0.150	0.150	0.150
error	0.100	0.100	0.100	0.100	0.100
Total dose rate, Gy/ka	**1.26**	**1.77**	**1.09**	**2.31**	**1.05**
error	**0.10**	**0.15**	**0.08**	**0.22**	**0.08**
% error	**8.08**	**8.40**	**7.61**	**9.37**	**7.53**

AGE (ka)	**105.80**	**107.83**	**121.62**	**24.21**	**55.41**
error	**16.71**	**11.53**	**11.74**	**3.47**	**7.56**
% error	**15.80**	**10.69**	**9.65**	**14.32**	**13.65**

	Whisby Quarry	Kirkby-on-Bain	Kirkby-on-Bain	Wellsyke Farm	Foxhill Pit
Sample number	**WHI05-02**	**KOB05-01**	**KOB05-02**	**WEL05-01**	**FOX05-01**
Laboratory code	**X2595**	**X2596**	**X2597**	**X2598**	**X2616**
Palaeodose (Gy)	51.88	26.96	36.83	260.23	247.30
uncertainty	3.089	3.977	4.827	14.711	8.425
measured	2.91	3.94	4.77	13.76	6.82
Systematic laboratory error (2 %)	1.038	0.539	0.737	5.205	4.946
Grain size					
Min. grain size (µm)	180	180	180	180	180
Max grain size (µm)	255	255	255	255	255
External gamma-dose (Gy/ka)	0.570	0.351	0.394	0.433	0.416
error	0.002	0.001	0.002	0.001	0.002
Measured concentrations					
standard fractional error	0.050	0.050	0.050	0.050	0.050
% K	1.200	0.780	0.760	1.300	1.100
error (%K)	0.060	0.039	0.038	0.065	0.055
Th (ppm)	4.400	2.700	2.600	1.600	1.400
error (ppm)	0.220	0.135	0.130	0.080	0.070
U (ppm)	1.200	0.600	0.500	0.500	0.400
error (ppm)	0.060	0.030	0.025	0.025	0.020
Cosmic dose calculations					
Depth (m)	1.250	6.400	2.500	1.050	6.000
error (m)	0.100	0.100	0.100	0.100	0.500
Average overburden density (g.cm^3)	1.900	1.900	1.900	1.900	1.900
error (g.cm^3)	0.100	0.100	0.100	0.100	0.100
Latitude (deg.), north positive	53	53	53	53	53
Longditude (deg.), east positive	1	0	0	0	0
Altitude (m above sea-level))	10	10	10	30	20
Cosmic dose rate (µGy/ka)	0.178	0.096	0.152	0.184	0.101
error	0.019	0.007	0.013	0.022	0.011
Moisture content					
Measured water content (%)	6.24	4.55	4.56	2.54	3.51
Estimated avearge water content	0.150	0.150	0.150	0.150	0.050
error	0.100	0.100	0.100	0.100	0.030
Total dose rate, Gy/ka	**1.66**	**1.02**	**1.09**	**1.46**	**1.34**
error	**0.13**	**0.08**	**0.08**	**0.12**	**0.07**
% error	**7.70**	**7.88**	**7.13**	**8.47**	**5.43**

AGE (ka)	**31.31**	**26.50**	**33.73**	**177.66**	**185.06**
error	**3.05**	**4.43**	**5.03**	**18.10**	**11.86**
% error	**9.74**	**16.72**	**14.92**	**10.19**	**6.41**

	Foxhill Pit	Langford	Langford	South Scarle	South Scarle
Sample number	**FOX05-02**	**LAN05-01**	**LAN05-02**	**SCI05-01**	**SCI05-02**
Laboratory code	**X2617**	**X2618**	**X2619**	**X2620**	**X2621**
Palaeodose (Gy)	259.08	38.54	38.70	93.37	57.97
uncertainty	10.186	2.933	1.950	8.488	10.971
measured	8.77	2.83	1.79	8.28	10.91
Systematic laboratory error (2 %)	5.182	0.771	0.774	1.867	1.159
Grain size					
Min. grain size (µm)	180	180	180	180	180
Max grain size (µm)	255	255	255	255	255
External gamma-dose (Gy/ka)	0.441	0.498	0.456	0.466	0.385
error	0.002	0.002	0.002	0.002	0.002
Measured concentrations					
standard fractional error	0.050	0.050	0.050	0.050	0.050
% K	1.240	0.890	1.240	0.960	0.900
error (%K)	0.062	0.045	0.062	0.048	0.045
Th (ppm)	1.400	2.800	2.100	5.300	3.200
error (ppm)	0.070	0.140	0.105	0.265	0.160
U (ppm)	0.400	0.800	0.600	1.900	1.300
error (ppm)	0.020	0.040	0.030	0.095	0.065
Cosmic dose calculations					
Depth (m)	5.200	6.600	6.300	1.820	1.250
error (m)	0.500	0.100	0.100	0.100	0.100
Average overburden density (g.cm^3)	1.900	1.900	1.900	1.900	1.900
error (g.cm^3)	0.100	0.100	0.100	0.100	0.100
Latitude (deg.), north positive	53	53	53	53	53
Longditude (deg.), east positive	0	1	1	1	1
Altitude (m above sea-level))	20	10	10	10	10
Cosmic dose rate (µGy/ka)	0.110	0.094	0.097	0.166	0.178
error	0.013	0.007	0.007	0.015	0.019
Moisture content					
Measured water content (%)	3.64	3.94	27.35	9.02	3.53
Estimated avearge water content	0.050	0.150	0.150	0.150	0.150
error	0.030	0.100	0.100	0.100	0.100
Total dose rate, Gy/ka	**1.47**	**1.25**	**1.38**	**1.48**	**1.28**
error	**0.08**	**0.09**	**0.12**	**0.12**	**0.10**
% error	**5.57**	**7.37**	**8.60**	**7.83**	**7.86**

AGE (ka)	**176.68**	**30.85**	**27.95**	**62.88**	**45.17**
error	**12.05**	**3.27**	**2.79**	**7.54**	**9.26**
% error	**6.82**	**10.59**	**9.97**	**12.00**	**20.49**

	Tattershall	Tattershall	Tattershall	Tattershall	Tattershall
Sample number	**TAT05-01**	**TAT05-02**	**TAT05-03**	**TAT05-04**	**TAT05-05**
Laboratory code	**X2622**	**X2623**	**X2624**	**X2625**	**X2626**
Palaeodose (Gy)	122.65	159.19	142.11	199.70	146.22
uncertainty	5.940	7.608	20.112	16.365	12.623
measured	5.41	6.91	19.91	15.87	12.28
Systematic laboratory error (2 %)	2.453	3.184	2.842	3.994	2.924
Grain size					
Min. grain size (µm)	180	180	180	180	180
Max grain size (µm)	255	255	255	255	255
					Mean
External gamma-dose (Gy/ka)	0.379	0.379	0.430	0.653	0.460
error	0.002	0.003	0.003	0.003	0.100
Measured concentrations					
standard fractional error	0.050	0.050	0.050	0.050	0.050
% K	0.800	0.650	0.600	1.620	1.000
error (%K)	0.040	0.033	0.030	0.081	0.050
Th (ppm)	1.800	2.800	3.000	6.300	2.200
error (ppm)	0.090	0.140	0.150	0.315	0.110
U (ppm)	0.500	0.800	0.900	1.500	0.600
error (ppm)	0.025	0.040	0.045	0.075	0.030
Cosmic dose calculations					
Depth (m)	4.320	3.900	3.400	2.900	2.600
error (m)	0.100	0.100	0.100	0.100	0.100
Average overburden density (g.cm^3)	1.900	1.900	1.900	1.900	1.900
error (g.cm^3)	0.100	0.100	0.100	0.100	0.100
Latitude (deg.), north positive	53	53	53	53	53
Longditude (deg.), east positive	1	1	1	1	1
Altitude (m above sea-level))	5	5	5	5	5
Cosmic dose rate (µGy/ka)	0.122	0.128	0.136	0.144	0.150
error	0.009	0.010	0.011	0.012	0.012
Moisture content					
Measured water content (%)	4.85	4.97	3.44	20.31	4.78
Estimated avearge water content	0.150	0.150	0.150	0.150	0.150
error	0.100	0.100	0.100	0.100	0.100
Total dose rate, Gy/ka	**1.06**	**1.02**	**1.06**	**2.02**	**1.30**
error	**0.08**	**0.07**	**0.07**	**0.17**	**0.14**
% error	**7.52**	**7.02**	**6.48**	**8.42**	**10.81**

AGE (ka)	**116.15**	**155.86**	**133.48**	**98.91**	**112.37**
error	**10.38**	**13.23**	**20.78**	**11.62**	**15.54**
% error	**8.94**	**8.49**	**15.57**	**11.75**	**13.83**

	Atkins Farm	Atkins Farm	Barrow	Besthorpe	Girton Quarry
Sample number	**ATK05-01**	**ATK05-02**	**BAR05-01**	**BES05-01**	**GIR05-01**
Laboratory code	**X2660**	**X2661**	**X2662**	**X2663**	**X2664**
	Unreliable very scattered	Unreliable very scattered			
Palaeodose (Gy)	*250.00*	*155.00*	16.92	28.77	20.64
uncertainty	20.616	20.239	4.273	2.868	1.402
measured	20.00	20.00	4.26	2.81	1.34
Systematic laboratory error (2 %)	5.000	3.100	0.338	0.575	0.413
Grain size					
Min. grain size (µm)	180	180	180	180	180
Max grain size (µm)	255	255	255	255	255
External gamma-dose (Gy/ka)	0.683	0.634	0.431	0.394	0.390
error	0.002	0.002	0.001	0.002	0.002
Measured concentrations					
standard fractional error	0.050	0.050	0.050	0.050	0.050
% K	1.130	0.950	1.200	0.950	0.850
error (%K)	0.057	0.048	0.060	0.048	0.043
Th (ppm)	3.000	2.900	2.600	2.100	1.400
error (ppm)	0.150	0.145	0.130	0.105	0.070
U (ppm)	0.900	0.900	2.100	0.800	0.500
error (ppm)	0.045	0.045	0.105	0.040	0.025
Cosmic dose calculations					
Depth (m)	1.100	1.350	2.500	10.500	4.000
error (m)	0.100	0.100	0.100	0.100	0.100
Average overburden density (g.cm^3)	1.900	1.900	1.900	1.900	1.900
error (g.cm^3)	0.100	0.100	0.100	0.100	0.100
Latitude (deg.), north positive	53	53	53	53	53
Longditude (deg.), east positive	1	1	1	1	1
Altitude (m above sea-level))	55	55	30	10	5
Cosmic dose rate (µGy/ka)	0.183	0.177	0.152	0.064	0.126
error	0.021	0.018	0.013	0.005	0.010
Moisture content					
Measured water content (%)	10.08	8.72	9.46	3.21	8.03
Estimated avearge water content	0.150	0.150	0.150	0.150	0.150
error	0.100	0.100	0.100	0.100	0.100
Total dose rate, Gy/ka	**1.68**	**1.52**	**1.55**	**1.14**	**1.09**
error	**0.12**	**0.10**	**0.13**	**0.10**	**0.08**
% error	**6.92**	**6.60**	**8.61**	**8.41**	**7.59**

AGE (ka)	**148.88**	**102.25**	**10.91**	**25.27**	**18.86**
error	**16.02**	**14.96**	**2.91**	**3.30**	**1.92**
% error	**10.76**	**14.63**	**26.68**	**13.05**	**10.18**

	Girton Quarry	Willington	Willington
Sample number	**GIR05-02**	**WIL05-01**	**WIL05-01**
Laboratory code	**X2665**	**X2666**	**X2667**
Palaeodose (Gy)	23.58	53.10	48.45
uncertainty	1.243	6.024	5.408
measured	1.15	5.93	5.32
Systematic laboratory error (2 %)	0.472	1.062	0.969
Grain size			
Min. grain size (µm)	180	180	180
Max grain size (µm)	255	255	255
External gamma-dose (Gy/ka)	0.396	0.419	0.404
error	0.002	0.002	0.002
Measured concentrations			
standard fractional error	0.050	0.050	0.050
% K	0.860	0.800	0.940
error (%K)	0.043	0.040	0.047
Th (ppm)	1.600	2.400	2.500
error (ppm)	0.080	0.120	0.125
U (ppm)	0.500	0.800	0.800
error (ppm)	0.025	0.040	0.040
Cosmic dose calculations			
Depth (m)	3.300	1.100	1.550
error (m)	0.100	0.100	0.100
Average overburden density (g.cm^3)	1.900	1.900	1.900
error (g.cm^3)	0.100	0.100	0.100
Latitude (deg.), north positive	53	53	53
Longditude (deg.), east positive	1	2	2
Altitude (m above sea-level))	5	40	40
Cosmic dose rate (µGy/ka)	0.137	0.183	0.172
error	0.011	0.021	0.017
Moisture content			
Measured water content (%)	3.68	7.32	6.28
Estimated avearge water content	0.150	0.150	0.150
error	0.100	0.100	0.100
Total dose rate, Gy/ka	**1.12**	**1.20**	**1.26**
error	**0.08**	**0.09**	**0.10**
% error	**7.52**	**7.16**	**7.72**

AGE (ka)	**21.03**	**44.30**	**38.54**
error	**1.93**	**5.94**	**5.23**
% error	**9.19**	**13.42**	**13.57**

Appendix 2: Dose rate determination

Radiation dose is measured in energy units of Gray (Gy), the standard SI unit of absorbed dose (1Gy = 1Joule/kg). The measurement of dose rate (or annual dose) can be made using a variety of different methods. For most samples, the majority of the environmental dose rate is due to the radioactive decay of unstable isotopes of potassium (K), uranium (U) and daughter isotopes, and thorium (Th) and daughter isotopes. A further small fraction comes from the cosmic dose rate, and is a function of altitude, geomagnetic latitude, and overburden thickness and density (Prescott and Hutton 1994). Water content attenuates the environmental dose rate, and uncertainties in the average of this value over the burial period may often form a significant contribution to the overall uncertainty in the age estimate.

In situ gamma spectrometry

Portable gamma spectrometer readings may be taken at each sampling location. The probe (housing an NaI scintillator crystal) is inserted into a deepened hole excavated following the retrieval of the OSL sample. Measurements typically take up to one hour and result in the direct estimation of the total *in situ* gamma radiation field. The spectra are also used to estimate contributions from U, Th, and K individually. Through comparison to known concentration standards, quantitative estimates of U, Th, and K concentrations are made.

ICP-MS analysis

A representative sub-sample (typically 10–20g, though as little as a few mg may be used with specialised procedures) of the OSL sample is sent for commercial analysis by fusion ICP-MS to an accredited laboratory. The fusion ensures that the entire sample is dissolved. It is only with this attack that major oxides including SiO2, REE and other high field strength elements are put into solution. The sample is first crushed to a nominal minus 10 mesh (1.7mm), mechanically split (riffle) to obtain a representative sample and then pulverized to at least 95% minus 150 mesh (106microns). Samples are prepared and analyzed in a batch system. Each batch contains a method reagent blank, certified reference material and 17% replicates. Samples are mixed with a flux of lithium metaborate and lithium tetraborate and fused in an induction furnace. The molten melt is immediately poured into a solution of 5% nitric acid containing an internal standard, and mixed continuously until completely dissolved (~30 minutes). The samples are run for major oxides and selected trace elements on a combination simultaneous/sequential Thermo Jarrell-Ash ENVIRO II ICP or a Spectro Cirros ICP. Calibration is performed using 7 prepared USGS and CANMET certified reference materials. One of the 7 standards is used during the analysis for every group of ten samples.Totals should be between 98.5% and 101%. If results come out lower, samples are scanned for base metals. Low reported totals may indicate sulphate being present or other elements like Li which won't normally be scanned for. Samples with low totals however are automatically refused and re-analyzed. The measurement of K and Th are usually precise, though samples with low levels of U may be below the detection limit for this element, depending on the interferences from other isotopes.

Moisture content of the sample

Moisture within the pore spaces of sediments absorbs α, β, and γ-radiation. As a result, less is absorbed by the mineral grains. It is therefore important to assess the present day water content of the sediment and to make some assessment of the variability of moisture throughout the burial period of the sample. The moisture correction factors outlined in Aitken (1985) and taken from Zimmermann (1971) are used in the age calculation (Appendix 1).

Cosmic dose rate

The contribution of cosmic radiation to the total dose rate is calculated as a function of (geomagnetic) latitude, altitude, burial depth, and average over-burden density, according to the formulae of Prescott and Hutton (1994).

Radiation attenuation factors

For coarse grains, the portion of the sample that receives an α-dose is removed by HF etching. Therefore, no consideration of the α-dose is made during the age calculation. β-particles (electrons) are significantly attenuated (ie a large fraction of the energy is absorbed) as the β-particle passes through a grain. Account of this effect is needed in order to correctly estimate the dose received by the 'average' grain. The so-called 'attenuation factors' are taken from the empirical work of Mejdahl (1979).

The γ-dose is assumed to be unaffected by attenuation as the penetration of gamma-rays through sediments is several orders of magnitude greater than (~10^5 times) the size of individual grains. Consequently, no attenuation factors are applied to the γ-dose.

Results for the U, Th (ppm), and K (%) concentration of each sample, together with the other parameters used in the age calculation, are provided in Appendix 1.

Appendix 3: Statistics and error calculation

The calculated age depends on the estimate of total absorbed dose (D_e) and the dose rate (D_R). Both of these estimates have uncertainties associated with them. This appendix gives general details of how the 'error' (the statistical uncertainty) is calculated for each term and combined with the errors on other terms to give an overall estimate of uncertainty on the OSL age estimate.

Palaeodose estimation

As described in a previous section (Fig 2.1), individual estimates of palaeodose also referred to as D_e are obtained from each of the aliquots (sub-samples) measured, using the SAR technique. The value of the D_e is obtained by interpolating between the points of the dose response curve. Statistical uncertainties are calculated for each of the individual points and also on the interpolated value of D_e. Typically, 12 aliquots are measured for each sample.

Each of the points on the growth curve is defined as:

$$I(\beta)_i = \frac{L_i - f \cdot l_i}{S_i - f \cdot s_i \cdot} \qquad \text{Equation 1}$$

where L_i is the integrated (initial) OSL from the regeneration dose and l_i is the measured background signal, S_i is the integrated (initial) OSL from the test dose (see Section 3) and s_i is the background; f is a scaling factor included to take account of the difference in duration of the L_i,S_i and l_i,s_i measurements.

The error on each dose-response data point (see Fig 2.1) is calculated by propagating 'counting statistics' errors (assuming Poisson statistics) from the integration of raw OSL data. The error on each term in Equation 1 is given by the square-root of the value. For example, the range for L_i is given by $L_i \pm \sqrt{L_i}$. The errors on each value are propagated in the standard way (see below) to give the uncertainty of $I(\beta)_i$.

In cases where the dose response can be (locally) approximated by a straight line, a weighted least squares linear fit is used. The errors in this case are calculated analytically using standard formulae.

In cases where the dose response is significantly non-linear, a single saturating exponential function is used to describe the dose response (a Simplex algorithm is used for fitting in this case). Occasionally an extra linear term is added to the exponential term in order to better describe the form of the dose response, although this is not commonly necessary. The uncertainty for non-linear fitting is calculated using a Monte-Carlo method in which 'random samples' of the dose response data are taken (assuming normally distributed probabilities) and used to obtain the palaeodose value. The spread in these values is then used to calculate the error on the mean palaeodose for each aliquot, giving a range for each palaeodose of $D_{ei} \pm \sigma D_{ei}$

Once the individual D_e values have been obtained from each aliquot (and the associated uncertainties calculated) the values are grouped to give a final overall estimate of D_e. The final D_e estimate is calculated using a weighted average. The weight of each D_e is referred to as w_i and defined as:

$$w_i = \frac{1}{\sigma D_{ei}{}^2} \Big/ \sum_i \frac{1}{\sigma D_{ei}{}^2} \qquad \text{Equation 2}$$

The weighted mean is defined as:

$$\overline{D}_e = \sum_i D_{ei} \cdot w_i \qquad \text{Equation 3}$$

The weighted standard error, $\hat{\sigma}_{\bar{x}w}$, is calculated from:

$$\hat{\sigma}_{\bar{x}w} = \sqrt{\frac{\sum_i w_i \left(D_{ei} - \overline{D}_e\right)}{1 - \frac{1}{n}}} \Bigg/ \sqrt{n} \qquad \text{Equation 4}$$

where n is the number of aliquots. The range of the weighted mean D_e is then defined as:

$$\overline{D}_e \pm \hat{\sigma}_{\bar{x}w} \qquad \text{Equation 5}$$

Slight modifications to the approach outlined above are made in special circumstances, though in most cases this description is sufficient.

Dose rate

The errors on the dose rate are due to errors in a range of values, for example, the concentration of U, Th, and K, as well as the water content of the sample. The individual components of the dose rate calculation are shown in Appendix 1. The uncertainty on the overall dose rate is calculated by combining the uncertainties according to the standard propagation formula given below.

Age calculation

The calculated age is obtained from dividing the mean palaeodose (Equation 3) by the total dose rate (Appendix 1). The uncertainty on the final age estimate is calculated using the error propagation formula given below. All calculations were performed using software developed within the laboratory.

Standard error propagation

If a calculated value (y) is calculated using a function (f) which contains terms x_1, x_2, x_3.... x_n , then,

$$y = f\left(x_1, x_2, x_3 \ldots x_n\right) \qquad \text{Equation 6}$$

Each term (x_i) has an associated uncertainty with a range expressed as $x_i \pm \sigma_{xi}$. The overall error of y can be calculated through the addition of the partial derivatives of y with respect to each term. Formally, this is written as:

$$\sigma_y = \sqrt{\sum_i \left(\frac{\partial y}{\partial x_i} \cdot \sigma_{xi} \right)^2} \qquad \text{Equation 7}$$

giving a range for y as $y \pm \sigma_Y$.